Gas-Phase Reactions of Nickel Oxide Clusters with Nitric Oxide. 1. Formation of Nitrogen Dioxide on Nickel Oxide Cluster Anions

W. D. Vann, R. L. Wagner, and A. W. Castleman, Jr.*

Department of Chemistry, Pennsylvania State University, 152 Davey Laboratory, University Park, Pennsylvania 16802

Received: August 11, 1997; In Final Form: December 10, 1997

A fast-flow reactor quadrupole mass spectrometer coupled with a laser vaporization source is used to study the gas-phase reactions of nickel oxide cluster anions $(Ni_xO_y)^-$ with nitric oxide (NO). The results show that nitrogen dioxide (NO_2) is formed on the nickel oxide clusters and that this formation leads to the loss of one or more species from the clusters in order to dissipate the heat of formation. The species lost from the clusters are nickel (Ni) and nickel oxide (NiO). Also, there is evidence that the association species of nitric oxide with nickel oxide anions rapidly form NO_2. Additional experiments were conducted in order to determine if this NO_2 formation mechanism is a function of how the nickel oxide cluster anions are formed. It was observed that a significantly different reaction occurs when nickel clusters are allowed to oxidize at room temperature and are then reacted with nitric oxide.

I. Introduction

Considerable interest has been shown over the past several years in developing more economical ways of dealing with harmful atmospheric pollutants that modern society generates. Among these pollutants are NO_x gases produced from combustion of fossil fuels. Heterogeneous catalytic processes are used by both the automobile industry and industrial manufacturers to remove these gases from their respective emission sources. Transition metals and their oxides play a major role in most catalytic processes used in industry today. Nickel, an important industrial catalyst, has been used for processes such as selective catalytic reduction (SCR) of NO_x gases from industrial emissions,[1] hydrogenation for the formation of methane,[2] and hydrogenolysis for the saturation of double bonds, benzene rings,[3] or carbonyl groups, as well as cracking processes.[2]

One promising approach to developing a greater understanding of catalytic processes is to study them on a molecular level through the use of clusters of varying stoichiometry, degree of aggregation, and oxidation state. These systems can function as molecular scale models of localized catalytic systems. Metal[4] and metal oxide[5] clusters, while not a perfect model of catalytic surfaces, can provide useful information on the short-range interactions occurring between a catalyst and reactant. Also in cases where catalytic surfaces are small, cluster chemistry will play a more direct role in understanding such systems. For example, cluster size metal particles smaller than 2 nm are used as catalysts in hydrocarbon reforming processes; also, small metal or metal oxide particles can be distributed in the micropores of zeolites.[6] Potential reaction mechanisms, reaction rates, competing reactions, and poisoning processes can be examined in detail through the use of cluster chemistry. The work described in this paper is part of an ongoing investigation designed to understand these types of interactions between nickel and nickel oxides catalysts and NO_x gases.

The present paper focuses on gas-phase reactions of nickel oxide cluster anions $(Ni_xO_y)^-$ with nitric oxide (NO) under well-defined thermal conditions. To study these reactions, nickel oxide clusters anions are produced by laser vaporization, reacted in a fast-flow reactor, and then detected by a quadrupole mass spectrometer. These experiments reveal new information on reactions and reaction mechanisms occurring between nickel oxide cluster anions and nitric oxide.

II. Experimental Section

The fast flow reactor mass spectrometer used in this work has been described in detail previously.[7] The continuous-flow laser vaporization source was modified from those previously employed[8] in order to produce cluster distributions with larger metal clusters. The design changes were modeled after work by deHeer et al.[9] The source was designed with a larger waiting room area, which allowed for less ion loss to the walls of the source. A rotating metal rod is vaporized in the presence of a flowing stream of carrier gas, and a small percentage of oxygen gas is mixed in with the carrier gas in order to form metal oxide clusters. The ablation species exit the source through a conical nozzle into the flow tube by way of a continuous flow of helium carrier gas (Air Products Specialty Gas, research grade 99.995%) at 9000 sccm (standard cubic centimeters per minute). The laser vaporization is performed using the second harmonic of a Nd:YAG laser (GCR-150, 30 Hz) focused onto a 0.6-cm nickel rod (Aldrich 99.5%) through a quartz window using a 20-cm focal length lens.

Upon entering the flow tube, ions are thermalized (296 K) by collisions with the carrier gas. The flow tube pressure is maintained at around 300 mTorr (monitored with a MKS 222B Baratron). To study the reactions of interest, neutral reactant gas (nitric oxide) is added through a reactant gas inlet (RGI) at a point in the flow tube where complete thermalization of the clusters is expected and laminar flow conditions are believed to exist. The reactants are allowed to react in the flow tube for a known amount of time before they are sampled and detected. The majority of the gas flowing through the reaction region is pumped off by a high-volume roots pump (Stokes Pennwalt model 1721), while a fraction of the ions is sampled from the flow through a 750 μm orifice and focused into the quadrupole mass filter (Extrel) by a set of electrostatic lenses. Thereafter,

S1089-5639(97)02617-0 CCC: $15.00
Published on Web 02/14/1998

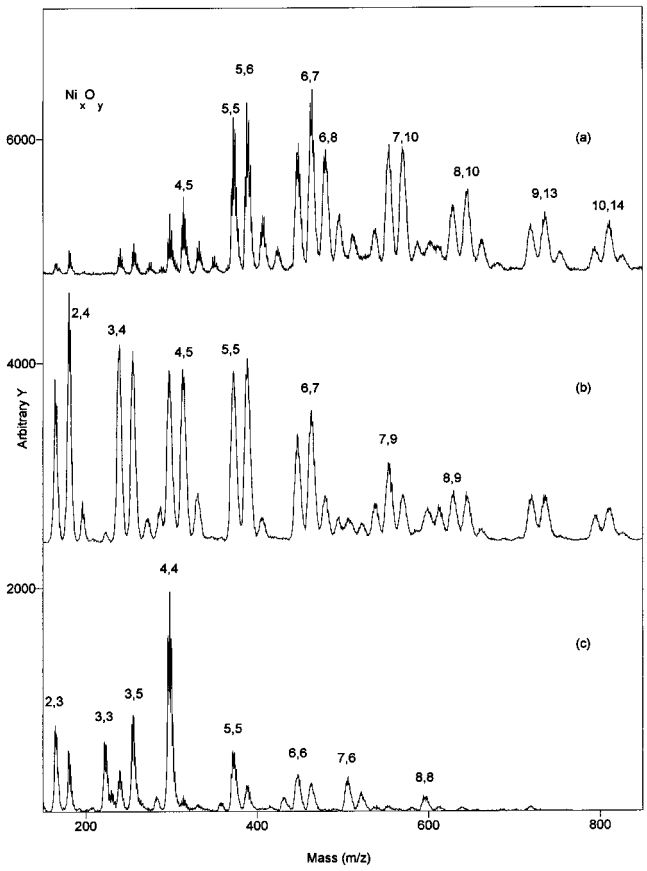

Figure 1. (a) Nickel oxide distribution produced from high-mass nickel clusters (produced at 4 mJ of 532-nm laser fluence) with 1 mTorr of O_2 in carrier gas. (b) Nickel oxide distribution from low-mass nickel oxide clusters (produced at 3−4 mJ) with 1 mTorr of O_2 in He. (c) Nickel oxide distribution produced when oxygen is added to the flow tube at 1 mTorr (4 mJ).

they are detected by a channeltron electron multiplier (Galileo model 4830). The quadrupole mass filter is controlled by a C-60 mass controller (Extrel). The quadrupole and detection chambers are differentially pumped, with pressures being maintained between 10^{-5} and 10^{-4} Torr. The pulsed output from the channeltron is fed through a pulse amplifier discriminator (Mech-Tronics Nuclear, 509) and then to a computerized multichannel analyzer (MCSII, Oxford Instruments).

III. Results

Nickel oxide cluster distributions were varied by changing experimental conditions within the laser vaporization source, such as the laser fluence or the percentage of oxygen in the carrier gas, as well as by varying the sampling orifice lens potentials. Figure 1 shows three different nickel oxide distributions; the major nickel oxide peaks found in the two upper distributions (Figure 1a,b) are assigned in Table 1. These are the species produced from the addition of oxygen at the source and range in composition from ones that are stoichiometric (1:1) to ones that are oxygen-rich. Nickel oxide clusters of similar stoichiometries are produced by adding oxygen to the flow tube, where the inherent high temperatures of the vaporization source are not encountered. However, there are several differences in these oxides compared with those formed in the source. First, a greater variety of oxides species are formed by adding oxygen at the source. When oxygen is added in the flow tube, the relative intensities favor nickel richer clusters (but still not nickel-rich with the exception of Ni_7O_6). The most striking difference is that the only nickel tetramer species produced is the Ni_4O_4 when oxygen is added to the flow tube, and it is considerably more prominent than the other oxide clusters. A possible explanation to this anomaly may be found when one considers the structure of the nickel tetramer as determined by corrected effective medium theory.[10] The structure of the nickel tetramer would allow the formation of a close-packed face-center-cubic arrangement as the four oxygen atoms bond at each of its four faces in such a way as to give the greatest degree of nickel−oxygen bonding without any rearrangement of the oxide cluster. Calculations to determine the structures of nickel oxide clusters would be helpful in understanding experimental distributions, but to date we are not aware of any such data in the literature. The most significant difference in the nickel oxides formed in the flow tube from those formed in the laser vaporization source, as far as this paper is concerned, is the fact that they react differently as will be discussed later in the paper.

TABLE 1: Assigned Composition of Observed Nickel Oxide Cluster Anions[a]

Ni_xO_x	Ni_xO_{x+1}	Ni_xO_{x+2}	Ni_xO_{x+3}	Ni_xO_{x+4}
			$Ni_{10}O_{13}$	$Ni_{10}O_{14}$
			794 amu	810 amu
			Ni_9O_{12}	Ni_9O_{13}
			720 amu	736 amu
	Ni_8O_9	Ni_8O_{10}	Ni_8O_{11}	
	612 amu	628 amu	644 amu	
	Ni_7O_8	Ni_7O_9	Ni_7O_{10}	
	538 amu	554 amu	570 amu	
Ni_6O_6	Ni_6O_7	Ni_6O_8		
448 amu	464 amu	480 amu		
Ni_5O_5	Ni_5O_6			
372 amu	388 amu			
Ni_4O_4	Ni_4O_5	Ni_4O_6		
298 amu	314 amu	330 amu		
	Ni_3O_4	Ni_3O_5	Ni_3O_6	
	240 amu	256 amu	272 amu	
	Ni_2O_3	Ni_2O_4	Ni_2O_5	
	164 amu	180 amu	196 amu	

[a] Nickel oxide clusters are arranged from stoichiometric to increasingly oxygen-rich clusters across the table, and from higher to lower mass down the table. The species listed in the table were produced by passing 1 mTorr of O_2 in He carrier gas over the nickel rod during the course of laser vaporization/ablation.

It is interesting to note from the data in Table 1 that in the source, only the tetramer, pentamer, and hexamer form oxides having stoichiometric compositions, while all other nickel containing cluster species are oxygen-rich. In the case of neutral clusters, a one-to-one clustering would produce an oxidation state of II, which is the most common oxidation state for nickel.[11] For anions, the oxidation state would change due to the excess electron on the cluster. Exact oxidation states, however, cannot be determined reliably without knowing the nature of the bonding within the clusters. Theoretical[12] and experimental[13] studies performed thus far help to shed some light on these oxidation processes, but still much work is needed to develop a full understanding of the formation of these nickel oxide clusters.

Using the two nickel oxide distributions given in Figure 1a,b as reactants, nitric oxide was added to the flow tube in various concentrations and allowed to react. For the reaction

$$Ni_xO_y^- + (NO)_z \rightarrow \text{product anions} + \text{neutrals} \qquad (1)$$

two product anion distributions are shown in Figure 2a,b.

The anion product distribution is quite complicated and requires a great deal of analysis in order to develop an

understanding of the processes occurring between the nickel oxide cluster anions and the neutral nitric oxide reactant molecules. It was first thought that the initial reaction might be just a simple association reaction between the metal oxide clusters and the nitric oxide. However, the product species do not consistently correspond to such a mass assignment. Indeed, there are peaks in the product distribution that cannot be accounted for by a simple association reaction. Those peaks marked by vertical lines in Figure 2 could not be accounted for either by the initial oxide species or by direct association of NO. Therefore, a different reaction mechanism had to be considered in order to explain these observations. Since many of the peak assignments corresponded to clusters with more oxygen than was present in the initial reactant oxide species, it was assumed that either the addition of oxygen to the clusters was enhanced by the association reaction with nitric oxide or reactions occurring on the surface of the cluster produced a loss of nickel and/or nickel oxide from the clusters. It is highly unlikely that NO association could enhance the addition of oxygen to the nickel oxide cluster anions since the oxides were already saturated prior to the addition of nitric oxide; hence, this possible mechanism can reasonably be eliminated from further consideration. The alternative mechanism would require a sufficient amount of energy to be gained in the association reaction in order to dissociate or break apart the cluster. However, it does not seem likely that a simple association could produce sufficient energy to break metal or metal oxide bonds in view of the much weaker bond character of an association complex as compared with metal or metal oxide bond strengths.

It is possible that another reaction is occurring at the cluster surface in combination with the association reaction, and it is this other reaction that yields sufficient energy to produce a loss of nickel and/or nickel oxide from the clusters. The product distributions indicate that there are reactions occurring on the cluster which produce nitrogen dioxide, suggesting an overall reaction mechanism as follows:

$$Ni_xO_y^- + NO \rightarrow (Ni_xO_y \cdot NO)^- \rightarrow (Ni_{x-1}O_{y-1\text{ or }2} \cdot NO_2)^- + Ni \quad \text{or} \quad NiO \quad (2)$$

$$(Ni_xO_y \cdot NO_2)^- + NO \rightarrow (Ni_xO_y \cdot NO_2 \cdot NO)^- \rightarrow (Ni_{x-1}O_{y-1\text{ or }2} \cdot (NO_2)_2)^- + Ni \quad \text{or} \quad NiO \quad (3)$$

$$(Ni_xO_y \cdot (NO_2)_2)^- + NO \rightarrow (Ni_xO_y \cdot (NO_2)_2 \cdot NO)^- \rightarrow (Ni_{x-1}O_{y-1\text{ or }2} \cdot (NO_2)_3)^- + Ni \quad \text{or} \quad NiO \quad (4)$$

$$(Ni_xO_y \cdot (NO_2)_3)^- + NO \rightarrow (Ni_xO_y \cdot (NO_2)_3 \cdot NO)^- \rightarrow (Ni_{x-1}O_{y-1\text{ or }2} \cdot (NO_2)_4)^- + Ni \quad \text{or} \quad NiO... \quad (5)$$

Evidence which indicates that the formation of NO_2 may have occurred from NO addition on metal oxides has been reported previously, for both iron oxide[14] and copper oxide.[15] Experiments on these and other metal oxides are currently underway in our laboratory.

IV. Analysis

To show that the mass assignment of the product peak distribution agrees with the NO_2 formation mechanism, a careful look at the possible product species is necessary. It is important to point out that for each of the $Ni_xO_y \cdot (NO_2)_z$ species discussed, the mass assignment could also be $Ni_xO_{y+z} \cdot (NO)_z$. However, in most cases this would give an oxide species with greater oxygen content than the original reactant oxides, and as

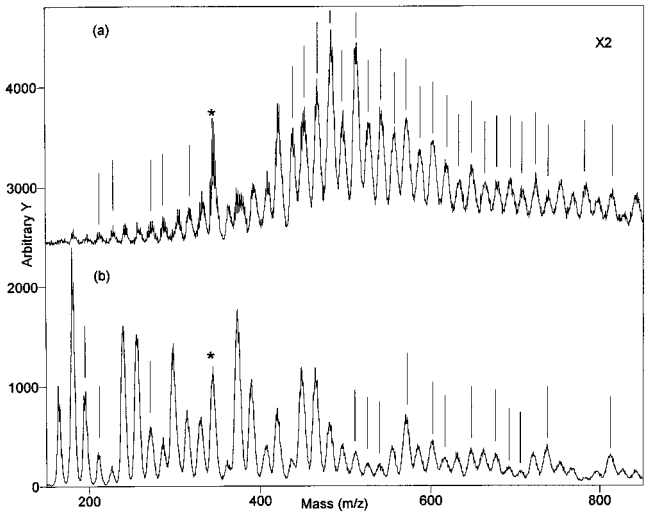

Figure 2. Product anion distribution from the reaction of nickel oxide clusters with (a) 5 sccm and (b) 2 sccm of NO, which correspond to the nickel oxide distributions in Figure 1a and 1b, respectively. Markings indicate peaks not accounted for by association of NO or starting material. Asterisk marks the $Ni_4O_4 \cdot (NO_2)$ species.

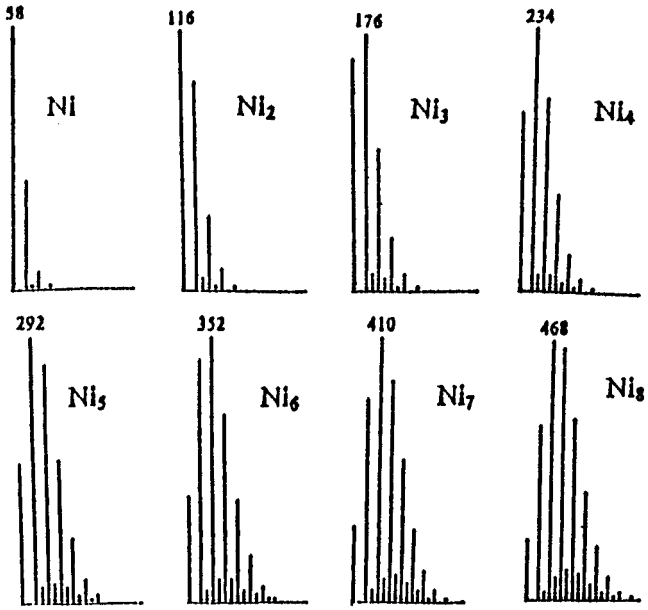

Figure 3. Isotopic distributions for Ni to Ni_8, with the mass of the most intense isotope labeled for each cluster. All other major isotopes within each cluster are 2 amu apart.

previously mentioned, this addition of oxygen to an association product cannot reasonably be explained. First, we will consider those peaks that cannot be explained by either the nickel oxide starting materials or the possible NO association products (i.e., discuss the peaks marked by the vertical lines in Figure 2). Then all the species that should be present with the NO_2 formation mechanism will be presented, regardless of whether they overlap with a nickel oxide or an association product. Much of this analysis is made possible by the different isotopic distributions found in nickel clusters. To help clarify this analysis, the isotopic distributions of Ni to Ni_8 are given in Figure 3. The oxygen and nitrogen have negligible effect on these distributions.

Figure 4 shows the possible NO_2 product species for the first region of the spectra that cannot be attributed to the starting material or an association product. In this figure a product distribution for the reaction of 2 sccm of NO is overlaid with the reactant oxide starting material distribution (dashed line) in

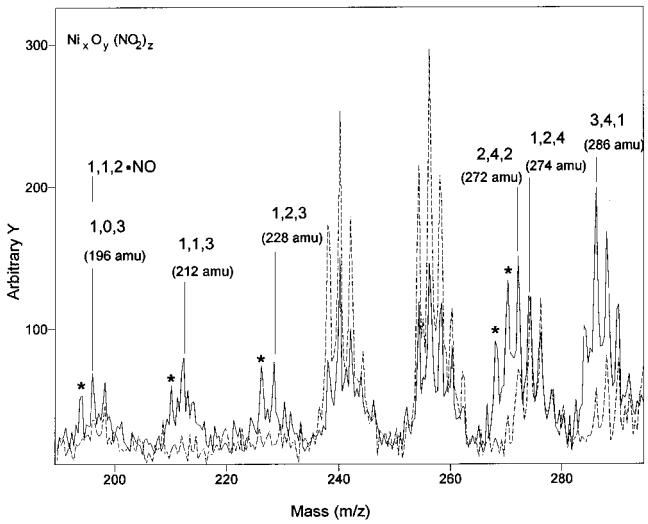

Figure 4. Product distribution for 2 sccm of NO overlaid with the reactant oxide distribution (dashed line), showing NO_2 formation species at peaks that cannot be attributed to either NO association complexes or remaining starting materials. The asterisks indicate peaks that are not part of the isotope pattern of the species labeled as discussed later in the text.

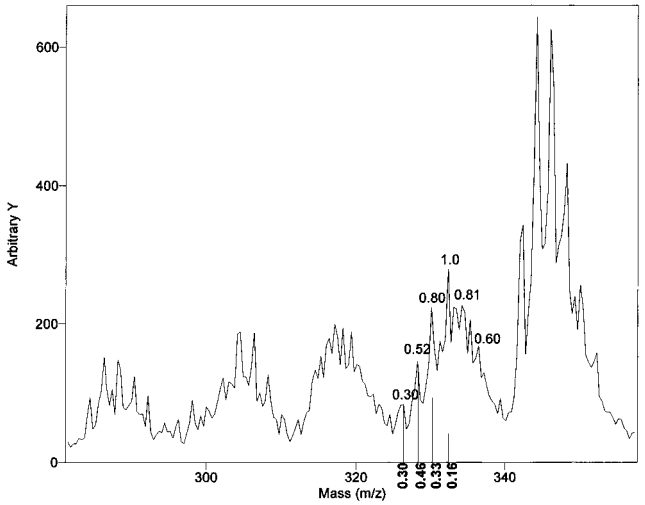

Figure 5. Enlarged section of product distribution, illustrating the method used for determining fraction of association products for each peak group as given in Table 2. The most intense peak in the group is set to 1, and the others are normalized to it. The lines indicate the isotope pattern of the Ni_4O_4•(NO) species.

order to show the growth of products and depletion of reactants. The product at mass 196 amu is seen in both distributions[16] and cannot be explained by attributing it to an association reaction product or a reactant. However, this species could be explained through the NO_2 formation mechanism by attributing it to the species Ni•$(NO_2)_3$ arising from the reaction of tetramer oxides through the losses of both Ni and NiO. It could also be assigned as being NiO•$(NO_2)_2$•NO, which would be part of the same mechanism. In a similar way, the tetramer oxides could also form the NiO•$(NO_2)_3$ species at mass 212, which again can only be explained by the NO_2 formation mechanism. Next, the 228-amu product seen in the higher mass data set (Figure 2a) could arise directly from the Ni_4O_5 reactant via the loss of Ni with each of the three reaction steps leading to NiO_2•$(NO_2)_3$.

The peak found at 272 amu has two possible explanations. First, there is a mass overlap from the Ni_3O_6 reactant, but this oxide is a minor reactant species and the observed signal at 272 amu grows larger with increasing NO concentration. Second, the NO_2 formation mechanism would lead to Ni_2O_4•$(NO_2)_2$ (mass 272) from the Ni_4O_6 reactant by the loss of Ni in each successive reaction step. Since this peak and the Ni_4O_6 oxide are both considerably stronger in the lower mass data set (Figure 2b), this could be an indication that the 272 peak comes from the Ni_4O_6 reactant. Next, there is some indication of the presence of a 274-amu species, which is attributable to NiO_2•$(NO_2)_4$. This species could be formed via the Ni loss channel from Ni_5O_6. The 286 peak is the Ni_3O_4•(NO_2) species, which could come either from the Ni_4O_6 reactant via one NiO loss or from the Ni_4O_5 reactant via one Ni loss.

Next, there is a large region in the product mass distributions where various NO_2 formation species completely overlap with the association or reactant species. This observation, however, does not indicate that there is no formation of the NO_2 species in this region of the mass spectra, a fact that can be shown by a careful comparison of the product distributions and the isotope patterns of possible products. For the purpose of discussion, we will define an isotopic peak group as a group of isotope peaks that are noticeably separated by low signal intensities or valleys in the product distributions. These isotopic peak groups are often combinations of more than one product species. To show that association products and original reactant species cannot fully account for the peaks in this region, the maximum possible fractions of each isotopic peak group in the spectra that could be attributed to the association species were calculated for the data set shown in Figure 2b. These calculated fractions were based on the isotope patterns of both the possible association species and the product peak groups seen in the spectra.

To calculate the percentage of association species that might be present, the intensities of each isotopic peak in the group were measured and compared with the isotopic ratios for the association product. The intensities of the association product isotopes were determined on the basis of their fit with the observed isotopic peak group and/or the intensities of the oxide precursor of the association product. These values are given in Table 2 for Ni_2O_y through Ni_6O_y. The first number given for each species of a given mass in the table is the maximum fraction of each peak group that could be attributed to the association product; the second number is the fraction of the reactant oxide peak that would have to be depleted in order to produce this amount of each of these association products.

To illustrate how these fractions are calculated, the isotope pattern of the Ni_4O_4•(NO) species is shown in Figure 5 (same mass as Ni_4O_3•(NO_2) species). First, the fit limiting peak from the observed peak group is determined. The fit limiting peak is the peak (from the peak group) that fits the nickel isotopic distribution the best without allowing the other isotopes to exceed the observed intensity at their respective masses. To determine this, the first isotope for Ni_4 is set to the observed peak intensity, and the fit of the remaining isotopes are noted. This process is repeated for each isotope of Ni_4, and the isotopic pattern that fits best without exceeding any of the observed peak intensities determines the limiting peak. In this instance the peak at 326 amu (first isotope shown in the isotopic pattern in Figure 5) limits the Ni_4O_4•(NO) fit to the observed peak group. Normalizing each of the peaks in this peak group to the 332-amu peak gives intensity values of 0.30, 0.52, 0.80, 1.00, 0.81, and 0.60 for 326, 328, 330, 332, 334, and 336 amu, respectively (labeled above each peak in Figure 5). With the 0.30 peak (326 amu) limiting the Ni_4O_4•(NO) fit, the remaining calculated values for the Ni_4O_4•(NO) are obtained from its isotopic ratio normalized to the first isotope (i.e., 1.0, 1.54, 1.09, 0.52).

TABLE 2: Considered Association Products for Ni_2O_y to Ni_6O_y

nickel oxide starting material	$Ni_xO_y(NO)$	$Ni_xO_y(NO)_2$	$Ni_xO_y(NO)_3$	$Ni_xO_y(NO)_4$	$Ni_xO_y(NO)_5$	$Ni_xO_y(NO)_6$
Ni_2O_3	194 amu	224 amu	254 amu	284 amu	314 amu	344 amu
	0.62	0.57	1	0.27	0.04	0
	0.75	0.09	0.61	0.30	0.07	0
Ni_2O_4	210 amu	240 amu	270 amu	300 amu	330 amu	360 amu
	0.15	0.18	0.03	0	0.06	0.09
	0.88	0.18	0.12	0	0.21	0.61
Ni_2O_5	226 amu	256 amu	286 amu	316 amu	346 amu	376 amu
	0.57	0	0.95	0.18	0.37	0
	0.30	0	0.59	0.09	0.11	0
Ni_3O_4	270 amu	300 amu	330 amu	360 amu	390 amu	420 amu
	0.25	0	0.37	0.15	0	0.44
	0.41	0	0.98	0.78	0	0.93
Ni_3O_5	286 amu	316 amu	346 amu	376 amu	406 amu	436 amu
	0.22	0	0.46	0.44	0.21	0.16
	0.77	0	0.43	0.20	0.92	0.69
Ni_3O_6	302 amu	332 amu	362 amu	392 amu	422 amu	452 amu
	0.53	1	0.94	0	1	1
	0.07	0.23	0.58	0	0.24	0.16
Ni_4O_4	328 amu	358 amu	388 amu	418 amu	448 amu	478 amu
	0.27	0.08	0.54	0.47	0.74	0.36
	0.43	0.40	0.62	0.59	0.81	0.57
Ni_4O_5	344 amu	374 amu	404 amu	434 amu	464 amu	494 amu
	0.76	1	0.20	0.10	0.74	0.26
	0.75	0.68	0.60	0.54	0.82	0.77
Ni_4O_6	360 amu	390 amu	420 amu	450 amu	480 amu	510 amu
	0.43	1	1	1	1	0.73
	0.88	0.32	0.49	0.35	0.51	0.70
Ni_5O_5	402 amu	432 amu	462 amu	492 amu	522 amu	552 amu
	0.42	0.09	0.62	0.20	0.12	0.20
	0.42	0.35	0.72	0.55	0.48	0.49
Ni_5O_6	418 amu	448 amu	478 amu	508 amu	538 amu	568 amu
	0.43	0.68	0.33	0.17	0.13	0.30
	0.71	0.89	0.63	0.60	0.66	0.50
Ni_6O_6	478 amu	508 amu	538 amu	568 amu	598 amu	628 amu
	0.43	0.29	0.22	0.31	0.25	0.34
	0.53	0.63	0.77	0.35	0.37	0.68
Ni_6O_7	494 amu	524 amu	554 amu	584 amu	614 amu	644 amu
	0.34	0.20	0.34	0.35	0.22	0.25
	0.86	0.71	0.77	0.75	0.60	0.57
Ni_6O_8	510 amu	540 amu	570 amu	600 amu	630 amu	660 amu
	0.85	0.54	1	1	0.80	0.78
	0.86	0.80	0.45	0.68	0.68	0.46

Multiplying 0.30 by 1.54, 1.09, and 0.52 gives the isotopic fits for 328, 330, and 332 amu, respectively (second, third, and fourth isotope shown in Figure 5). By summing the isotopic fit values (0.30, 0.46, 0.33, and 0.16 labeled below each isotope in Figure 5) and dividing by the sum of the observed values (0.30, 0.52, 0.80, 1.0, 0.81, and 0.60), the maximum possible fraction of $Ni_4O_4 \cdot (NO)$ contribution is determined to be 0.31. This example is taken from the high-mass data set (Figure 2a), in order to show how these fractions varied from one data set to the next. The values given in Table 2 are from the low mass data set (Figure 2b), and for the $Ni_4O_4 \cdot (NO)$ the larger value of 0.43 was reported. It was consistently observed throughout the data sets that the low-mass data generated higher fractions (as seen in this example) for each of the possible association species.

The data from the table indicates that over half of the association products account for less than 60% of each of the peaks in the spectra, and 90% of them leave 20% or more of the peaks unaccounted for. These numbers may appear somewhat small until one considers that the fractions of the association products given are only maximum values and that the actual values would be less because the association product isotope patterns rarely fit the observed product isotopic peak group correctly. This point can be further illustrated by summing the fractions of the reactant oxide depleted in order to form each of the association species for any one of the oxide reactants (i.e., summing the second fraction for each nickel oxide starting material across any one entire row in Table 2). All but one oxide reactant, the Ni_2O_4, were depleted more than 100%, and in many cases the depletion is well over 200%, indicating that the fractions of the association products presented are grossly overestimated. The point here is that even with these grossly overestimated fractions of association products, there is still a considerable amount of the various spectra that cannot be accounted for by simple association reactions. Also if one were to sum the intensities of all the possible association products listed in Table 2 for each peak group, there would still be considerable discrepancies in the product distributions.

In the second half of the product distributions (400−800 amu), there are many more peaks that cannot be due to nitric oxide association. This could be an indication that the larger nickel oxide clusters promote the NO_2 formation reaction more readily than do the smaller clusters. The first NO_2 cluster in this larger mass region that has no possible mass overlap with an association product is the $Ni_4O_7 \cdot (NO_2)_2$ species at mass 438 amu. This cluster is shown in Figure 6 and is believed to originate from the Ni_6O_9 oxide cluster via two reaction steps, each involving a nickel loss. It is also possible that the $Ni_3O_2 \cdot (NO_2)_5$ species contributes to the peak group found at mass 438, which comes from either the Ni_8O_{10} or the Ni_8O_{11}

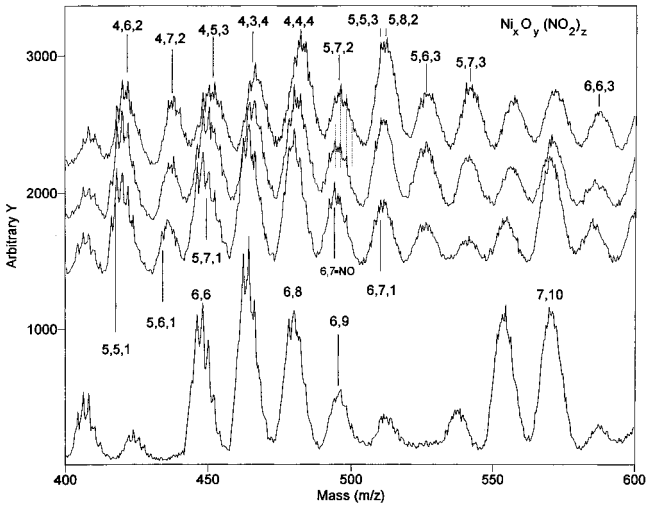

Figure 6. Progression of NO_2 formation reaction with increasing NO concentration (from bottom to top: 0, 1, 3, 5 sccm of NO). Isotopic pattern for the pentamer is shown by the dotted line in the top trace. Species can be observed to shift from starting material (Ni_6O_6, Ni_6O_7, Ni_6O_8, ...) to a single reaction steps ($Ni_5O_5{\cdot}(NO_2)$, $Ni_5O_6{\cdot}(NO_2)$, $Ni_5O_7{\cdot}(NO_2)$, ...) and further with increasing NO concentration to multiple reaction steps ($Ni_4O_6{\cdot}(NO_2)_2$, $Ni_4O_7{\cdot}(NO_2)_2$, $Ni_4O_5{\cdot}(NO_2)_3$, ...).

TABLE 3: Possible NO_2 Formation Mechanism Species Produced from Ni_3O_x[a]

Ni		Ni_3O_4	$Ni_2O_2(NO_2)$
loss ↓		240 amu	194 amu
	Ni_3O_5	$Ni_2O_3(NO_2)$	$NiO(NO_2)_2$
	256 amu	210 amu	166 amu
Ni_3O_6	$Ni_2O_4(NO_2)$	$NiO_2(NO_2)_2$	
272 amu	226 amu	182 amu	
$Ni_2O_5(NO_2)$	$NiO_3(NO_2)_2$		
242 amu	198 amu		
$NiO_4(NO_2)_2$		NiO	
214 amu		loss →	

[a] Across the table represents NiO loss reactions, and down the table represents Ni loss.

TABLE 4: Possible NO_2 Formation Mechanism Species Produced from Ni_4O_x[a]

Ni		Ni_4O_4	$Ni_3O_2(NO_2)$	$Ni_2(NO_2)_2$
loss ↓		298 amu	254 amu	208 amu
	Ni_4O_5	$Ni_3O_3(NO_2)$	$Ni_2O(NO_2)_2$	
	314 amu	270 amu	224 amu	
Ni_4O_6	$Ni_3O_4(NO_2)$	$Ni_2O_2(NO_2)_2$	$Ni(NO_2)_3$	
330 amu	286 amu	240 amu	196 amu	
$Ni_3O_5(NO_2)$	$Ni_2O_3(NO_2)_2$	$NiO(NO_2)_3$		
302 amu	256 amu	212 amu		
$Ni_2O_4(NO_2)_2$	$NiO_2(NO_2)_3$			
272 amu	228 amu			
$NiO_3(NO_2)_3$		NiO		
244 amu		loss →		

[a] Across the table represents NiO loss reactions, and down the table represents Ni loss.

reactant through five reaction steps and different combinations of Ni and NiO losses. Figure 6 shows, for the mass region from 400 to 600 amu, the progressive steps of the NO_2 formation mechanism as NO concentration is increased. The bottom trace shows the nickel oxide starting material, while each successive trace has a higher NO concentration added (1, 3, and 5 sccm). All traces are on the same scale, with the top three offset for clarity. All possible NO_2 cluster products for this region are not labeled due to the lack of space, but are given in Tables 3−10. The progressive steps for the NO_2 formation can be seen in many of the peak groups shown in this region. The first two labeled peaks illustrate this point well, where the $Ni_5O_5{\cdot}(NO_2)$ species at mass 418 shifts with increasing NO concentration to the $Ni_4O_6{\cdot}(NO_2)_2$ species at mass 422 amu. This progression can also be seen with the $Ni_5O_6{\cdot}(NO_2)$ species (434 amu) shifting to the $Ni_4O_7{\cdot}(NO_2)_2$ species (mentioned previously), as well as Ni_6O_6 species (448 amu) shifting to the $Ni_5O_7{\cdot}(NO_2)$ species (450 amu) and then further to the $Ni_4O_5{\cdot}(NO_2)_3$ species (452 amu). Each of these shifts represents an increased number of reaction steps arising due to higher reactant concentrations.

TABLE 5: Possible NO_2 Formation Mechanism Species Produced from Ni_5O_x[a]

Ni	Ni_5O_5	$Ni_4O_3(NO_2)$	$Ni_3O(NO_2)_2$
loss ↓	372 amu	328 amu	284 amu
Ni_5O_6	$Ni_4O_4(NO_2)$	$Ni_3O_2(NO_2)_2$	$Ni_2(NO_2)_3$
388 amu	344 amu	300 amu	254 amu
$Ni_4O_5(NO_2)$	$Ni_3O_3(NO_2)_2$	$Ni_2O(NO_2)_3$	
360 amu	316 amu	270 amu	
$Ni_3O_4(NO_2)_2$	$Ni_2O_2(NO_2)_3$	$Ni(NO_2)_4$	
332 amu	286 amu	242 amu	
$Ni_2O_3(NO_2)_3$	$NiO(NO_2)_4$		
302 amu	258 amu		
$NiO_2(NO_2)_4$		NiO	
274 amu		loss →	

[a] Across the table represents NiO loss reactions, and down the table represents Ni loss.

In the region from 450 to 500 amu, there are three peaks that can only be accounted for by clusters containing NO_2, namely, the 466, 482, and 496-amu peaks. Each of these peaks are the predominant ones found in the isotopic patterns and are at least 2 amu higher than any possible association product peaks that might be considered as contributing by mass overlap. The 466-amu peak can be attributed to the $Ni_5O_8{\cdot}(NO_2)$ and the $Ni_4O_3{\cdot}(NO_2)_4$ species. The $Ni_5O_8{\cdot}(NO_2)$ cluster is produced by a single reaction step commencing from the Ni_6O_9 reactant by the loss of one Ni from the cluster. The $Ni_4O_3{\cdot}(NO_2)_4$ species comes from either the Ni_8O_{11} (four reaction steps, all NiO losses) or the Ni_8O_{10} (four steps, three NiO and one Ni loss). Evidence will be given later that will indicate that this species would more likely be $Ni_4O_4{\cdot}(NO_2)_3{\cdot}NO$, which would come from Ni_7O_9 or Ni_7O_{10}. The 482-amu peak comes from the $Ni_4O_4{\cdot}(NO_2)_4$ species, which would come from the same reactants as the $Ni_4O_3{\cdot}(NO_2)_4$ species, with one Ni loss replacing one NiO loss.

At this point, it becomes redundant to continue to name the reaction steps and the loss channels for each product since they all follow the same mechanism. One can determine the number of reaction steps (s) simply by the number of NO_2 species in the cluster. It is also apparent that the number of nickels found in the starting material is equal to the sum of the Ni and NO_2 species in the cluster. The possible loss channels are not always as straightforward but can be determined in the following manner

$$\text{for} \quad Ni_xO_y \quad \text{and} \quad Ni_{x-s}O_z{\cdot}(NO_2)_s$$

$$L_{Ni} = z + 2s - y \tag{6a}$$

$$\text{and} \quad L_{NiO} = s - L_{Ni} \tag{6b}$$

where L_{Ni} is the number of nickel losses and L_{NiO} is the number of NiO losses.

The peak at 496 amu has two likely mass assignments attributable to the NO_2 formation mechanism, namely, $Ni_5O_7{\cdot}(NO_2)_2$ and $Ni_5O_4{\cdot}(NO_2)_3$. There is, however a third less likely mass assignment at 496 amu, the $Ni_4O_2{\cdot}(NO_2)_5$ species (less likely because of five reaction steps), which would have a slightly different isotope pattern than the nickel pentamer

TABLE 6: Possible NO_2 Formation Mechanism Species Produced from Ni_6O_x[a]

Ni				Ni_6O_6	$Ni_5O_4(NO_2)$	$Ni_4O_2(NO_2)_2$
loss ↓				448 amu	402 amu	358 amu
			Ni_6O_7	$Ni_5O_5(NO_2)$	$Ni_4O_3(NO_2)_2$	$Ni_3O(NO_2)_3$
			464 amu	418 amu	374 amu	330 amu
		Ni_6O_8	$Ni_5O_6(NO_2)$	$Ni_4O_4(NO_2)_2$	$Ni_3O_2(NO_2)_3$	$Ni_2(NO_2)_4$
		480 amu	434 amu	390 amu	346 amu	300 amu
	Ni_6O_9	$Ni_5O_7(NO_2)$	$Ni_4O_5(NO_2)_2$	$Ni_3O_3(NO_2)_3$	$Ni_2O(NO_2)_4$	
	496 amu	450 amu	406 amu	362 amu	316 amu	
Ni_6O_{10}	$Ni_5O_8(NO_2)$	$Ni_4O_6(NO_2)_2$	$Ni_3O_4(NO_2)_3$	$Ni_2O_2(NO_2)_4$		
512 amu	466 amu	422 amu	378 amu	332 amu		
$Ni_5O_9(NO_2)$	$Ni_4O_7(NO_2)_2$	$Ni_3O_5(NO_2)_3$	$Ni_2O_3(NO_2)_4$			
482 amu	438 amu	394 amu	348 amu			
$Ni_4O_8(NO_2)_2$	$Ni_3O_6(NO_2)_3$	$Ni_2O_4(NO_2)_4$	$NiO_2(NO_2)_5$			
454 amu	410 amu	364 amu	320 amu			
$Ni_3O_7(NO_2)_3$	$Ni_2O_5(NO_2)_4$	$NiO_3(NO_2)_5$				
426 amu	380 amu	336 amu		NiO loss →		

[a] Across the table represents NiO loss reactions, and down the table represents Ni loss.

TABLE 7: Possible NO_2 Formation Mechanism Species Produced from Ni_7O_x[a]

Ni	Ni_7O_9	$Ni_6O_7(NO_2)$	$Ni_5O_5(NO_2)_2$	$Ni_4O_3(NO_2)_3$	$Ni_3O_1(NO_2)_4$
loss ↓	554 amu	510 amu	464 amu	420 amu	376 amu
Ni_7O_{10}	$Ni_6O_8(NO_2)$	$Ni_5O_6(NO_2)_2$	$Ni_4O_4(NO_2)_3$	$Ni_3O_2(NO_2)_4$	$Ni_2(NO_2)_5$
570 amu	526 amu	480 amu	436 amu	392 amu	346 amu
$Ni_6O_9(NO_2)$	$Ni_5O_7(NO_2)_2$	$Ni_4O_5(NO_2)_3$	$Ni_3O_3(NO_2)_4$	$Ni_2O(NO_2)_5$	
542 amu	496 amu	452 amu	408 amu	362 amu	
$Ni_5O_8(NO_2)_2$	$Ni_4O_6(NO_2)_3$	$Ni_3O_4(NO_2)_4$	$Ni_2O_2(NO_2)_5$		
512 amu	468 amu	424 amu	378 amu		
$Ni_4O_7(NO_2)_3$	$Ni_3O_5(NO_2)_4$	$Ni_2O_3(NO_2)_5$			
484 amu	440 amu	394 amu			
$Ni_3O_6(NO_2)_4$	$Ni_2O_4(NO_2)_5$		NiO		
456 amu	410 amu		loss →		

[a] Across the table represents NiO loss reactions, and down the table represents Ni loss.

TABLE 8: Possible NO_2 Formation Mechanism Species Produced from Ni_8O_x[a]

Ni	Ni_8O_{10}	$Ni_7O_8(NO_2)$	$Ni_6O_6(NO_2)_2$	$Ni_5O_4(NO_2)_3$	$Ni_4O_2(NO_2)_4$	$Ni_3(NO_2)_5$
loss ↓	628 amu	584 amu	540 amu	496 amu	450 amu	406 amu
Ni_8O_{11}	$Ni_7O_9(NO_2)$	$Ni_6O_7(NO_2)_2$	$Ni_5O_5(NO_2)_3$	$Ni_4O_3(NO_2)_4$	$Ni_3O(NO_2)_5$	
644 amu	600 amu	556 amu	510 amu	466 amu	422 amu	
$Ni_7O_{10}(NO_2)$	$Ni_6O_8(NO_2)_2$	$Ni_5O_6(NO_2)_3$	$Ni_4O_4(NO_2)_4$	$Ni_3O_2(NO_2)_5$		
616 amu	572 amu	526 amu	482 amu	438 amu		
$Ni_6O_9(NO_2)_2$	$Ni_5O_7(NO_2)_3$	$Ni_4O_5(NO_2)_4$	$Ni_3O_3(NO_2)_5$			
588 amu	542 amu	498 amu	454 amu			
$Ni_5O_8(NO_2)_3$	$Ni_4O_6(NO_2)_4$	$Ni_3O_4(NO_2)_5$				
558 amu	514 amu	470 amu				
$Ni_4O_7(NO_2)_4$	$Ni_3O_5(NO_2)_5$			NiO		
530 amu	486 amu			loss →		

[a] Across the table represents NiO loss reactions, and down the table represents Ni loss.

TABLE 9: Possible NO_2 Formation Mechanism Species Produced from Ni_9O_x

Ni		Ni_9O_{12}	$Ni_8O_{10}(NO_2)$	$Ni_7O_8(NO_2)_2$	$Ni_6O_6(NO_2)_3$	$Ni_5O_4(NO_2)_4$
loss ↓		720 amu	674 amu	630 amu	586 amu	540 amu
	Ni_9O_{13}	$Ni_8O_{11}(NO_2)$	$Ni_7O_9(NO_2)_2$	$Ni_6O_7(NO_2)_3$	$Ni_5O_5(NO_2)_4$	$Ni_4O_3(NO_2)_5$
	736 amu	690 amu	646 amu	602 amu	556 amu	512 amu
Ni_9O_{14}	$Ni_8O_{12}(NO_2)$	$Ni_7O_{10}(NO_2)_2$	$Ni_6O_8(NO_2)_3$	$Ni_5O_6(NO_2)_4$	$Ni_4O_4(NO_2)_5$	$Ni_3O_2(NO_2)_6$
752 amu	706 amu	662 amu	618 amu	572 amu	528 amu	484 amu
$Ni_8O_{13}(NO_2)$	$Ni_7O_{11}(NO_2)_2$	$Ni_6O_9(NO_2)_3$	$Ni_5O_7(NO_2)_4$	$Ni_4O_5(NO_2)_5$		
722 amu	678 amu	634 amu	588 amu	544 amu		
$Ni_7O_{12}(NO_2)_2$	$Ni_6O_{10}(NO_2)_3$	$Ni_5O_8(NO_2)_4$	$Ni_4O_6(NO_2)_5$			
694 amu	650 amu	604 amu	560 amu			
$Ni_6O_{11}(NO_2)_3$	$Ni_5O_9(NO_2)_4$	$Ni_4O_7(NO_2)_5$				
666 amu	620 amu	576 amu				
$Ni_5O_{10}(NO_2)_4$			NiO			
636 amu			loss →			

[a] Across the table represents NiO loss reactions, and down the table represents Ni loss.

species; mixing of isotopic patterns makes it difficult to completely discount this possible product. This peak group at 496 amu has been fit with a nickel pentamer isotope pattern indicated by the dotted lines under the 5 sccm trace (top spectra in Figure 6). From a careful comparison of isotope patterns for products and reactant oxides at this mass region (492−500 amu) and the peak group observed in the spectra, it becomes apparent that there is some other species (other than $Ni_5O_7{\cdot}(NO_2)_2$, and $Ni_5O_4{\cdot}(NO_2)_3$) at mass 494 amu. Two possible explanations can account for this: first, the isotopic pattern of the Ni_6O_9 species has a strong peak at 494 amu, but it would be weaker than the 496 peak (0.91 of the peak at 496). The 1-sccm trace

TABLE 10: Possible NO_2 Formation Mechanism Species Produced from $Ni_{10}O_x$[a]

Ni loss ↓		$Ni_{10}O_{13}$ 794 amu	$Ni_9O_{11}(NO_2)$ 750 amu	$Ni_8O_9(NO_2)_2$ 704 amu	$Ni_7O_7(NO_2)_3$ 660 amu	$Ni_6O_5(NO_2)_4$ 616 amu
	$Ni_{10}O_{14}$ 810 amu	$Ni_9O_{12}(NO_2)$ 766 amu	$Ni_8O_{10}(NO_2)_2$ 720 amu	$Ni_7O_8(NO_2)_3$ 676 amu	$Ni_6O_6(NO_2)_4$ 632 amu	$Ni_5O_4(NO_2)_5$ 586 amu
$Ni_{10}O_{15}$ 826 amu	$Ni_9O_{13}(NO_2)$ 782 amu	$Ni_8O_{11}(NO_2)_2$ 736 amu	$Ni_7O_9(NO_2)_3$ 692 amu	$Ni_6O_7(NO_2)_4$ 648 amu	$Ni_5O_5(NO_2)_5$ 602 amu	$Ni_4O_3(NO_2)_6$ 558 amu
$Ni_9O_{14}(NO_2)$ 798 amu	$Ni_8O_{12}(NO_2)_2$ 752 amu	$Ni_7O_{10}(NO_2)_3$ 708 amu	$Ni_6O_8(NO_2)_4$ 664 amu	$Ni_5O_6(NO_2)_5$ 618 amu	$Ni_4O_4(NO_2)_6$ 574 amu	
$Ni_8O_{13}(NO_2)_2$ 768 amu	$Ni_7O_{11}(NO_2)_3$ 724 amu	$Ni_6O_9(NO_2)_4$ 680 amu	$Ni_5O_7(NO_2)_5$ 634 amu	$Ni_4O_5(NO_2)_6$ 590 amu		
$Ni_7O_{12}(NO_2)_3$ 740 amu	$Ni_6O_{10}(NO_2)_4$ 696 amu	$Ni_5O_8(NO_2)_5$ 650 amu	$Ni_4O_6(NO_2)_6$ 606 amu		NiO loss →	

[a] Across the table represents NiO loss reactions, and down the table represents Ni loss.

shows the 494 peak as being stronger than the 496 peak, indicating that the Ni_6O_9 species cannot fully account for this peak at this lower concentration. The second explanation for the 494-amu peak would be the presence of a small amount of Ni_6O_7·NO species (an association product), which could account for this anomaly in the lower concentration data set, especially considering that this would be the first step in the NO_2 formation mechanism from the Ni_6O_7 starting material.

The remaining section of product distributions (500−800 amu) contains 15 different peaks that cannot be explained by a simple association mechanism but can be attributed to the NO_2 formation mechanism. In fact, this region gives some of the strongest evidence supporting the NO_2 formation mechanism. For instance, consider the 512-amu peak. It is the most intense peak in its isotopic group, and the closest possible association product would be Ni_6O_8·(NO) (which, incidentally, is part of the NO_2 formation mechanism) at 510 amu. Normalizing the 512 peak to unity (i.e. dividing each peak intensity by the peak intensity of the 512 peak), the intensity of the 508 peak becomes 0.665, and the 510 peak is 0.972. On the basis of the isotopic distribution of Ni_6, the 508 peak would be the limiting factor in determining the contribution made to the 512 peak by Ni_6O_8·(NO). Of the possible association products, this one (based on its isotope pattern) would make the largest contribution to the 512 peak. From this, it can be determined that if the 508 comes solely from Ni_6O_8·(NO), then the calculated intensities for this association species would be 0.730 for 510 amu and 0.526 for 512 amu, leaving a considerable amount of peak intensity unaccounted for by NO association. The NO_2 formation mechanism has many possibilities that could account for these discrepancies, such as Ni_5O_8·$(NO_2)_2$ and Ni_4O_3·$(NO_2)_5$ centered at mass 512 amu, as well as Ni_6O_7·(NO_2), Ni_5O_5·$(NO_2)_3$, and Ni_4O_6·$(NO_2)_4$ centered at 510, 510, and 514 amu respectively (see Figure 6).

Each of the next 14 peaks can be evaluated in a similar manner with the same results. Most of the possible association products fall at least 2 mass units off-center of each isotopic peak group, limiting their possible contribution to it. Each of these peak groups has one or more possible explanations from the NO_2 formation mechanism that are centered on that peak group. Also, there are several other species off-center that could contribute to that particular isotopic peak group. To better illustrate the contribution of these off-center species, consider the peaks for the monomer and dimer nickel clusters labeled in Figure 4. Nickel monomer has a strong isotope at 58 amu (normalized to 1), a weaker peak at 60 amu (0.38), and a much smaller isotope at 62 amu (0.05). Nickel dimer has a strong isotope at 116 amu (normalized to 1) and two other significant isotopes at 118 amu (0.76) and 120 amu (0.25). From this, and the observed isotopic distributions in Figure 4, it becomes apparent that the peaks to the left (marked with asterisks) of each of those assigned in the figure cannot be explained by any of the labeled monomer and dimer species. In each case, to fully account for the entire isotopic peak group, it must be considered to come from isotopic mixing of various products, some of which would be off-centered. Evidence of the NO_2 formation mechanism is apparent throughout the entire product distribution. All the possible NO_2 cluster species formed through this mechanism are given in the Tables 3−10, where Ni loss channels are represented down the table and NiO loss channels are listed across the table.

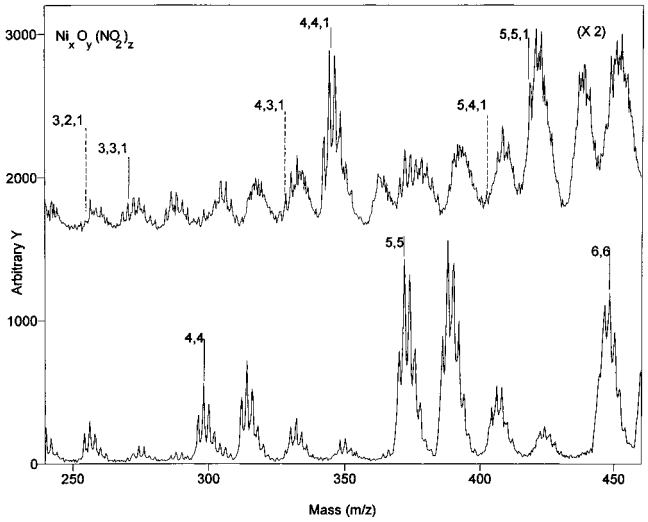

Figure 7. (lower trace) Nickel oxide reactant species. (upper trace) Nickel-rich products (dashed lines) from the NiO loss channels and the stoichiometric oxides (solid lines) produced from the Ni loss channel.

V. Discussion

The considerable amount of mass overlap is the major problem in determining which of the NO_2 cluster species are most prominent or which reaction channels are more favorable. It is apparent that many of the species listed in Tables 3−10 are not prominent contributing species, particularly those species with four or more reaction steps. It is possible that only the first few reaction steps from each reactant oxide are taking place. Depending on the oxygen content of the clusters, it is possible that they may follow a preferred loss channel. This point is well-illustrated by the data given in Figure 7, which shows the reactant oxides in the lower trace and the NO_2 cluster products in the upper trace. The three NiO loss products, which produce metal-rich clusters, are marked by the dashed lines; the Ni loss products, which form stoichiometric nickel oxide clusters, are marked by the solid lines. These three NiO loss products were chosen because there is no other possible formation channel and very little, if any, possible mass overlap with the starting

material. The $Ni_5O_4{\cdot}(NO_2)$ species centered at 402 amu is a very minor peak, accounting for at most 28% of the product peak near that mass. This NO_2 species could arise from the Ni_6O_6 oxide via one NiO loss; in other words, the reactant cluster would have to break a NiO bond to form NO_2 and retain the Ni atom while losing a NiO to form a nickel-rich oxide cluster. If one assumes that nickel oxides do not prefer to form nickel-rich clusters (in accordance with what has been observed experimentally[17]), then it is reasonable to expect that the formation of $Ni_5O_4{\cdot}(NO_2)$, would be a minor reaction channel. Another example of the same process is found for the $Ni_3O_2{\cdot}(NO_2)$ species (254 amu) which is a negligible peak in the high mass region data set. The low mass data set has a significant mass overlap at 256 amu from the Ni_3O_5 reactant that makes it impossible to determine how much, if any, $Ni_3O_2{\cdot}(NO_2)$ species is present. Considering then the high-mass data, which has very little Ni_3O_5 to mask any NO_2 formation channel, it becomes apparent that the NiO loss channel is not the mechanism followed in this case. In both of these cases the Ni loss product (which allows the cluster to remain a stoichiometric oxide) is the prominent product. This truncation of the NO_2 formation mechanism at a stoichiometric oxide can be explained if one considers the possible oxidation states of nickel in the cluster; the mixed valence of the cluster under nickel-rich conditions would require one or more nickels to be monovalent, which is not a preferred oxidation state for nickel.

If one now considers the 402-amu peak group and assigns it to be the association product $Ni_5O_5{\cdot}(NO)$, the question then arises as to why this species is not prominent in the product distribution. The same question arises with the possible $Ni_4O_4{\cdot}(NO)$ species. There was sufficient Ni_5O_5 and Ni_4O_4 to form these association product (there was no Ni_3O_3 to allow the formation of the $Ni_3O_3{\cdot}(NO)$ species). This would seem to provide rather convincing evidence that the association species are minor contributors to the product distributions and that the NO_2 formation occurs very quickly and leaves little trace of the initial association species. At least this is evidently the case for $Ni_5O_5{\cdot}(NO)$ and $Ni_4O_4{\cdot}(NO)$ association products. More evidence in support of the possibility that NO association species convert quickly to NO_2 can be found by comparing the differences in the reactant oxide distributions from the two data sets in Figure 2 and then looking at how these differences affect the product distributions. The peak at 344 amu (see peaks marked with asterisks in Figure 2) was assigned to be the $Ni_4O_4{\cdot}(NO_2)$ species. If it were an association product, it would be the $Ni_4O_5{\cdot}(NO)$ species. These are the only mass assignments that fit 344 amu. The Ni_4O_5 oxide starting material is twice as strong in the low-mass data set (Figure 1b) as it is in the high-mass set (Figure 1a). It is then reasonable to assume that some noticeable difference would be seen in the products formed from these two oxides. The product peaks, however, are of approximately equal intensities as are the Ni_5O_5 and Ni_5O_6 oxide starting materials that would have produced the $Ni_4O_4{\cdot}(NO_2)$ species. This may be an oversimplification of what could be a very complicated process, but at the lowest concentration of NO where one would expect the first reaction stages (i.e., the NO association) to occur, this inequality of reactants consumed versus products created still exists for the NO association scheme. This provides further evidence that NO association is occurring only to a limited extent.

On the basis of the observations that both clusters with four or more reaction steps and nickel-rich clusters are less prominent, these NO_2 product species were removed from consideration and the remaining products listed in the Tables 3−10 were reevaluated in order to determine if all the peaks in the spectra could be accounted for by these remaining species. In doing this, it was found that all but a few of the peaks in the spectra could easily be accounted for. Those peaks, or more precisely parts of peaks that could not be accounted for, could be assigned to single NO associations either to the bare nickel oxide clusters or to NO_2/nickel oxide cluster. Again these species are a necessary part of the reaction mechanism. Two examples of this are the $NiO{\cdot}(NO_2)_2{\cdot}NO$ and the $Ni_3O_6{\cdot}(NO_2)_3{\cdot}NO$ species at masses 196 and 440 amu, respectively. The 196-amu assignment was mentioned previously. The 440-amu peak was only apparent in the spectra where the maximum concentration of NO reactant was employed in obtaining the high-mass data set. From this species, the reaction mechanism would yield $Ni_2O_5{\cdot}(NO_2)_4$ or $Ni_2O_4{\cdot}(NO_2)_4$, which would be the completion of the fourth reaction step. This may indicate that the NO_2 formation mechanism slows as more reaction steps occur and begins to give way to the formation of association products. Also this may be another indication that smaller nickel clusters do not react as readily as larger ones to form NO_2.

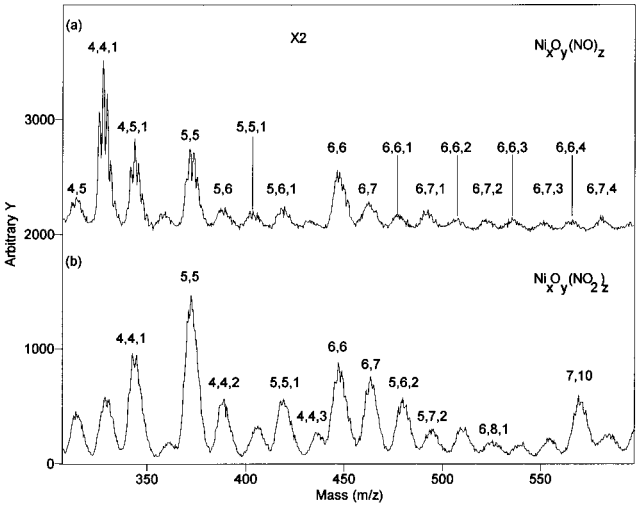

Figure 8. Comparison of product distributions for 3 sccm of NO reacted with both nickel oxides formed in the flow tube (a) and nickel oxides formed in the laser vaporization source (b). The lower spectrum (b) shows the NO_2 formation product distribution as has been discussed in the text with a few of the product species labeled. The upper spectrum (a), however, shows a product distribution that corresponds to NO association products. The peaks labeled in the upper spectrum (a) are for $Ni_xO_y{\cdot}(NO)_z$, while the peaks labeled in spectrum b are for $Ni_xO_y{\cdot}(NO_2)_z$.

To determine if the NO_2 formation mechanism is a function of the way the oxide clusters are formed, in another series of experiments nickel oxide clusters were produced by adding oxygen to the flow tube well upstream from the reactant gas inlet (see Figure 1c). This was accomplished by adding oxygen to the nickel clusters which were (by this point in the flow tube) thermalized to room temperature by collisions with the He carrier gas. Figure 8 shows a comparison of the data sets for the reaction of NO with $Ni_xO_y^-$ produced with nickel oxide clusters formed in the flow tube (Figure 8a) and from the oxides produced at the vaporization source (Figure 8b). Both spectra show the products for the addition of 3 sccm of NO. However, considerably different products are formed by these two oxide distributions. The main difference is that the species produced from the nickel oxide clusters formed in the flow tube can be accounted for by the simple association of NO with a nickel oxide cluster. The peaks labeled in Figure 8a are for association products $Ni_xO_y{\cdot}(NO)_z$. Such association products were previously considered and discussed for the product distribution

shown in Figure 8b (NO_2 formation species), and were shown to be inconsistent. A few of the peaks in Figure 8b have been labeled ($Ni_xO_y \cdot (NO_2)_z$) to show the difference between the two distributions. At this concentration, a single NiO loss channel forms a $Ni_6O_8 \cdot (NO_2)$ from the Ni_7O_{10}, and a second reaction step produces the $Ni_5O_7 \cdot (NO_2)_2$ and $Ni_5O_6 \cdot (NO_2)_2$ utilizing both loss channels (Ni and NiO). Finally a third reaction step yields the formation of $Ni_4O_4 \cdot (NO_2)_3$ (4,4,3 in the figure) through the NiO loss channel. Other $Ni_xO_y \cdot (NO_2)_z$ species labeled show first and second reaction steps from the Ni_6O_6, Ni_6O_7, and Ni_5O_5 species.

In Figure 8a the formation of association products is quite apparent, with consecutive additions of nitric oxide starting from the nickel oxide clusters. It is necessary to point out that there is a mass overlap in the NO association assignments given in Figure 8a for the $Ni_6O_6 \cdot (NO)_2$ and the $Ni_6O_7 \cdot (NO)_2$ with Ni_7O_6 and Ni_7O_7, respectively. This means that while it is most likely that $Ni_6O_6 \cdot (NO)_2$ and the $Ni_6O_7 \cdot (NO)_2$ are labeled correctly, the $Ni_6O_6 \cdot (NO)_3$ and the $Ni_6O_7 \cdot (NO)_3$ could very well be, in part, $Ni_7O_6 \cdot (NO)$ and the $Ni_7O_7 \cdot (NO)$, and so on. The exact assignment is not what is important here, but rather the fact that these species are NO association products. There is, however, one species in the product distribution in Figure 8a that is somewhat difficult to explain. This peak is centered at mass 344 amu which would correspond to and is labeled as $Ni_4O_5 \cdot (NO)$ (4,5,1 in the figure), but there is no Ni_4O_5 starting material (mass 314). This then could correspond to $Ni_4O_4 \cdot NO_2$, but why would this particular species form NO_2? There is a small peak at 314 amu after the addition of NO, which would indicate that the peak at 344 amu is a simple addition of one NO to this peak, suggesting that there is little or no NO_2 formation occurring, mainly the simple addition of NO. The species formed at mass 314 amu could be Ni_4O_5 or any combination of $Ni_3O_5 \cdot (NO)_2$, $Ni_3O_3 \cdot (NO)_3$, and $Ni_2O_3 \cdot (NO)_5$, which are possible NO association products. The main point is that for the most part these nickel oxide clusters formed in the flow tube produce NO association products. This is quite puzzling, considering the reactant oxide distributions have many similarities. In trying to develop a clearer understanding of why these two oxide distributions give different products, we looked carefully at the similarities. For instance, the reaction rate (which will be published in part 2 of this study) for the Ni_4O_4 reaction with NO is much faster for the oxides formed in the flow tube. If the reaction rates of these two Ni_4O_4 species had been the same, one could suggest that they do react the same and the differences in the product distributions are due to the differences in the reactant distributions. This, however, is not the case. The question is no longer do they really react differently, but why do they react so differently?

Further experiments were conducted in order to observe the nickel oxide build-up pattern in both types of nickel−oxygen clusters, and some very significant differences were observed. A 1% dilution of oxygen in helium was introduced, either through the source or the reactant gas inlet of the flow tube, by a flow controller, in order to obtain precise flow rates. As the flow rate (i.e., concentration of oxygen) was gradually changed, the build-up patterns of the two different types of oxides could be seen. When oxygen is added to the source, a very smooth build-up pattern is observed, with distinct single oxygen atom additions. When oxygen is added to the flow tube, no smooth build-up pattern is observed. For instance, the trimer appears to form Ni_3O_2 and then Ni_3O_3, where the latter becomes the predominate trimer oxide species. The tetramer goes directly to the Ni_4O_2 and then to Ni_4O_4 with very little Ni_4O_3 being formed, and, as can be seen in Figure 1c, the Ni_4O_4 is the predominate tetramer oxide. The pentamer's build-up pattern shows the Ni_5O_3 and Ni_5O_5 to be the main oxides formed with very little Ni_5O_2 or Ni_5O_4 being formed. The formation of nickel−oxygen clusters in the flow tube seems to be produced through the addition of both single oxygen atoms and oxygen molecules. This may be the key to understanding why these species react differently than the nickel oxides formed in the source. It is reasonable to expect that nickel and oxygen would bond to form different structures when produced in the source, where nickel and oxygen are believed to cluster simultaneously, as opposed to the structures formed when oxygen is reacted with fully formed and thermalized nickel clusters. The latter might give rise to species comprised of oxygens bound to the nickel atoms without fully disrupting all of the metal−metal bonds, because metal−oxygen bonds are stronger than metal−metal bonds,[18] while the formation of fully oxidized metal structures would likely be produced by the intense reactions in the source.

To address how the NO_2 formation may be occurring, an understanding of catalytic metal and metal oxide surfaces must be employed and extrapolated down to the cluster regime. Surface studies show that in transition metal oxides, the electronegativity of oxygen causes the metal to take on a slightly Lewis acid character (electron pair acceptor) by withdrawing electrons from the metal.[19] With nickel acting as a Lewis acid in the cluster, this would facilitate the bonding of the nitrogen (of the nitric oxide) to the nickel atoms. This may explain why the nitric oxide does not react to form nitrogen dioxide on the surface of the oxide clusters that were formed in the flow tube. These oxide clusters would tend to associate or attach oxygen to the outside of the previously formed nickel clusters, which might increase the likelihood of nitric oxide bonding to the oxygen rather than the metal atoms of the cluster, allowing only an association product.

Recent nickel oxide surface studies indicate that NO bonds nitrogen down.[20] Additionally, back-bonding by overlap of nickel d-orbitals with the π^* antibonding orbital of the NO would further weaken the nitrogen−oxygen bond of nitric oxide. This same back-bonding process of d-electrons into the π^* antibonding orbitals of the adsorbate molecule has been reported for CO with nickel and other transition metals.[21,22] This weakening of the nitrogen oxygen bond would help to facilitate a second oxygen to bond to nitrogen to form NO_2. However, the presence of oxygen may reduce the ability of the d-electrons to back-bond with the NO, by reducing the electron density of the metal atoms. If this is the case, the strength of the nickel−nitrogen bond may be the sole influence responsible for the weakening of the nitrogen−oxygen bond. It is also possible that a side-on type bonding to the cluster surface is occurring, where the electron density shift caused by the nickel−nitrogen bonding may help facilitate the bonding of the NO oxygen to a nickel, stretching the NO bond and promoting NO_2 formation. Near-edge X-ray-absorption fine structure studies have indicated that the molecular axis of NO adsorbed onto a NiO surface is tilted approximately 45° relative to the surface normal.[21]

The three major differences in this study compared to other surface-type studies are the extra electron on the anionic clusters, the presence of excess oxygen in the cluster above the one-to-one ratio found in bulk nickel oxides, and the coordinately unsaturated nature of the atoms in the cluster, each of which could play a role in the NO_2 formation mechanism. The electron on the nickel oxide cluster would significantly increase the local electron density at the reaction center, causing a much stronger

back-bonding effect, and the electron affinity of the NO oxygen may enhance bonding to the electron-rich cluster. Also, if the electron is more localized at a lower coordinated oxygen, this would increase the likelihood of that oxygen bonding with NO to form NO_2. This could explain why the formation mechanism truncates at stoichiometric nickel oxide clusters. Also the occurrence of the truncation itself implies that the excess oxygen definitely plays an important role in the formation mechanism. However, this is certainly not the only factor responsible for the formation of NO_2; in cation experiments, which will be published separately, the presence of excess oxygen is not sufficient to facilitate the formation of NO_2.

The reactivity of the anion clusters may also be enhanced by the degree to which atoms in the cluster are coordinately unsaturated. This also may be more comparable to defect, corner, and edge sites, which are believed to be more reactive than surface sites. Comparing nickel oxide clusters to these coordinately unsaturated sites, and carefully considering how the excess electron and oxygen affect the reaction center, is expected to lead to a greater understanding of processes occurring at transition metal oxide surfaces such as these and aid in developing enhanced catalytically active surfaces.

VI. Conclusion

The main intent of this paper is to show that NO_2 is formed on nickel oxide clusters (produced by laser vaporization in the presence of oxygen) and this formation leads to the loss of one or more nickel-containing species from the clusters. The nickel oxides formed by introducing oxygen at the vaporization source are stoichiometric or oxygen-rich clusters. These clusters, when reacted with nitric oxide, produce nitrogen dioxide at the cluster surface through one or more reaction steps. To dissipate the energy produced from the formation of NO_2, one or more of the species are released from the cluster. Among the possible loss species are Ni and NiO. Preferred loss mechanisms are those that allow the nickel oxides to remain stoichiometric or oxygen-rich. Evidence indicates that, at these reactant gas concentrations, the reaction terminates after three or four formation steps (at higher NO concentrations more reaction steps may occur) and that it is possible the NO association species are rapidly converted to NO_2, leaving little trace of them in the product distribution.

Acknowledgment. Financial support by the Division of Chemical Sciences, Office of Basic Energy Sciences, Office of Energy Research of the U.S. Department of Energy, Grant No. DE-FGO2-92-ER14258, is gratefully acknowledged.

References and Notes

(1) Bosch, H.; Janssen, F. *Catal. Today* **1988**, *2*, 369.
(2) Somorjai, G. A. *Introduction to Surface Chemistry and Catalysis*; John Wiley & Sons, Inc.: New York, 1994.
(3) Augustine, R. L. *Heterogeneous Catalysis for the Synthetic Chemist*; Marcel Dekker, Inc.: New York, 1996.
(4) (a) Riley, S. E. In *Metal Ligand Interactions: From Atoms, to Clusters, to Surfaces*; Salahub, D. R.; Russo, N., Eds.; Kluwer Academic Press: Dordrecht, 1992; pp 17−36. (b) Eller, K.; Schwarz, H. *Chem. Rev.* **1991**, *91*, 1121.
(5) Shröder, D.; Schwarz, H. *Angew. Chem., Int. Ed. Engl.* **1995**, *34*, 1973.
(6) (a) van Santen, R. A. *Theoretical Heterogeneous Catalysis*; World Scientific: River Edge, NJ, 1991. (b) Sano, M.; Suzuki, M.; Niwa, M. *Bull. Chem. Soc. Jpn.* **1993**, *66*, 3511.
(7) Castleman, A. W., Jr.; Weil, K. G.; Sigsworth, S. W.; Leuchtner, R. E.; Keesee, R. G. *J. Chem. Phys.* **1987**, *86*, 3829.
(8) Leuchtner, R. E.; Harms, A. C.; Castleman, A. W., Jr. *J. Chem. Phys.* **1990**, *92*, 6527.
(9) deHeer, W. A.; Milani, P. *Rev. Sci. Instrum.* **1990**, *61*, 1835.
(10) Stave, M. S.; DePristo, A. E. *J. Chem. Phys.* **1992**, *97*, 3386.
(11) Cotton, F. A.; Wilkinson, G. *Advanced Inorganic Chemistry a Comprehensive Text*, 3rd ed.; John Wiley & Sons, Inc.: New York, 1972.
(12) Grimes, R. W.; Onwood, D. *J. Chem. Soc., Faraday Trans.* **1990**, *86*, 233.
(13) (a) Nieman, G. C.; Parks, E. K.; Richtsmeier, S. C.; Lui, K.; Pobo, L. G.; Riley, S. J. *High Temp. Sci.* **1986**, *22*, 115. (b) Reetz, M. T.; Quaiser, S. A.; Winter, M.; Becker, J. A.; Schäfer, R.; Stimming, U.; Marmann, A.; Vogel, R.; Konno, T. *Angew. Chem., Int. Ed. Engl.* **1996**, *35*, 2092.
(14) Busca, G.; Lorenzelli, V. *J. Catal.* **1981**, *72*, 303.
(15) London, J. W.; Bell, A. T. *J. Catal.* **1973**, *31*, 32.
(16) The high-mass data set (Figure 1a) showed 196 amu only at 1−3 sccm of NO.
(17) Nickel reacts with oxygen even in extremely small concentrations (0.5 cc in 9000 cc of He), forming stoichiometric to oxygen-rich species. Metal-rich species can be produced only in the presence of extremely small concentrations of oxygen (from 0.1 up to 0.5 cc in 9000 cc of He).
(18) For example: (a) Gingerich, K. A. In *Metal Bonding and Interactions in High Temperature Systems with Emphasis on Alkali Metals*; Gole, J. L., Stwalley, W. C., Eds.; American Chemical Society: Washington, DC, 1982; pp 109−123. (b) Conrad, H.; Ertl, G.; Kuppers, J.; Latta, E. *Surf. Sci.* **1975**, *50*, 296.
(19) Madix, R. J. In *Oxygen Complexes and Oxygen Activation by Transition Metals*; Martell, A. E., Sawyer, D. T., Eds.; Plenum Press: New York, 1988; pp 253−264.
(20) Kuhlenbeck, H.; Odörfer, G.; Jaeger, R.; Illing, G.; Menges, M.; Mull, Th.; Freund, H.-J.; Pöhlchen, M.; Staemmler, V.; Witzel, S.; Scharfschwerdt, C.; Wennemann, K.; Liedtke, T.; Neumann, M. *Phys. Rev. B* **1991**, *43*, 1969.
(21) *Ibach, H.; Somorjai, G. A. Appl. Surf. Sci.* **1979**, *3*, 293. Dubois, L. H.; Zegrarski, B. R. *Chem. Phys. Lett.* **1985**, *120*, 537.
(22) White, M. G. *Heterogeneous Catalysis*; Prentice Hall: Englewood Cliffs, NJ, 1990.